Excitations of a Bose-Einstein condensate in a one-dimensional optical lattice

J.-P. Martikainen* and H. T. C. Stoof†
Institute for Theoretical Physics, Utrecht University, Leuvenlaan 4, 3584 CE Utrecht, The Netherlands
(Received 15 April 2003; published 24 July 2003)

We investigate the low-lying excitations of a stack of weakly coupled two-dimensional Bose-Einstein condensates, which is formed by a one-dimensional optical lattice. In particular, we calculate the dispersion relations of the monopole and quadrupole modes, both for the ground state as well as for the case in which the system contains a vortex along the direction of the lasers creating the optical lattice. Our variational approach enables us to determine analytically the dispersion relations for an arbitrary number of atoms in every two-dimensional condensate and for an arbitrary momentum. We also discuss the feasibility of observing our results experimentally.

DOI: 10.1103/PhysRevA.68.013610 PACS number(s): 03.75.Kk, 32.80.Pj, 03.65.−w

I. INTRODUCTION

Cold bosons in an optical lattice provide a uniquely tunable environment to explore quantum phenomena. Some of these phenomena have been known theoretically for quite some time, but with the advent of new experimental tools they have become a focus of attention. For example, Bloch oscillations of electrons in a metal are a standard material in condensed-matter text books, but advances in the manipulation of cold atoms have also made their experimental investigation possible in this case [1]. In addition, diffraction of matter waves by a pulsed optical lattice was studied by Ovchinnikov *et al.* [2]. Optical lattices have also enabled the observation of some more exotic quantum phenomena such as number squeezing [3] and collapses and revivals [4]. Apart from these examples, Bose-Einstein condensates in optical lattices are particularly promising physical systems to study superfluid properties of Bose gases [5,6]. Very importantly, they realize the Bose-Hubbard model [7] and can be used to investigate the quantum phase transition from the superfluid into a Mott-insulator state [7,8]. This phase transition was recently indeed observed experimentally [9].

In this paper we present a variational method to study the excitations in a stack of weakly coupled two-dimensional (quasi)condensates. Such a system can be created by applying a relatively strong one-dimensional optical lattice to an ordinary three-dimensional condensate. We focus on the transverse monopole and quadrupole modes, but we also demonstrate how the method can be applied to study longitudinal excitations. We determine the eigenfrequencies of the monopole and quadrupole modes without any other approximations than those involved in our variational ansatz. In particular, this means that we can smoothly cross over from the noninteracting limit to the Thomas-Fermi regime. Moreover, the longitudinal wavelength of the modulation is arbitrary, i.e., nearest-neighbor sites can be completely out of phase. Using typical experimental parameters, we predict that the dispersion relations show a strong dependence on the lattice potential.

We consider the transverse excitations both for the ground state of the gas, as well as for the case that a vortex pierces through the center of each two-dimensional (quasi)condensate. We also consider the latter case, because a recent experiment observed the transverse vibrational modes of the vortex line in a trapped Bose-Einstein condensate. These modes are called Kelvin modes [10]. In the lattice, three-dimensional effects (such as vortex line curvature), are expected to be less important. Therefore, we believe that the Kelvin modes, and in particular their coupling to the transverse collective modes, are easier to study in a lattice than in a cigar-shaped three-dimensional condensate. Our results for a stationary vortex represent the first necessary step towards understanding the more complicated problem of the Kelvin modes of a vortex in an optical lattice.

There is a number of important theoretical papers on the dynamics of Bose-Einstein condensates in optical lattices. For example, dynamical and modulational instabilities were studied in Refs. [11–13] and the adiabaticity of the nonlinear wave equations was explored by Band and Trippenbach [14]. Massignan and Modugno derived [15] a relatively simple way to solve the three-dimensional Gross-Pitaevskii equation and used it to investigate the dynamics and expansion of the condensate in a one-dimensional optical lattice. Finally, Krämer *et al.* [16] used hydrodynamic equations to study the low-lying collective modes of a harmonically trapped Bose-Einstein condensate in the presence of a one- or two-dimensional optical lattice. In particular, they showed that the effect of the lattice is to renormalize the interaction coupling constant and introduce an effective mass that accounts for the different inertia along the lattice potential. With these changes, it is, for instance, possible to apply the results for harmonically trapped condensates obtained by Stringari [17].

The study by Krämer *et al.* is somewhat related to ours. The most important difference, however, is that Krämer *et al.* are interested in different modes than we are. They deal with low-energy excitations along the long axis of the cigar-shaped condensate, i.e., the longitudinal modes. In the absence of a magnetic trap, they correspond to the Bogoliubov modes with the familiar phonon spectra at large wavelengths. In the presence of a harmonic trap the spectrum becomes discrete, and the lowest energetic modes are the center-of-mass mode and the (longitudinal) quadrupole mode. The

*Electronic address: J.P.J.Martikainen@phys.uu.nl
†Electronic address: stoof@phys.uu.nl

transverse modes we are interested in have superfluid flows orthogonal to the long axis of the condensate. Moreover, in the z direction along the lasers of the optical lattice the condensate is, for simplicity, treated as completely periodic. As we see later, we take in first instance the atom number in each two-dimensional (quasi)condensate to be constant and equal in every site. This removes the Bogoliubov modes from the excitation spectrum, since they correspond to a density modulation propagating along the z axis. If desired, they can, however, be easily incorporated into our approach. Indeed, at the end of the paper we briefly discuss the corresponding sound mode when the atom number in each two-dimensional (quasi)condensate is allowed to fluctuate.

There are several experiments on condensates in a one-dimensional optical lattices [1,5,6,18–20], but none of these address the problem we consider in this paper. Fort *et al.* [20] measured longitudinal excitation frequencies of the condensate in the presence of a one-dimensional optical lattice, and this is the experimental paper most closely related to our work. In particular, for the breathing mode Fort *et al.* [20] do not report any dependence on the lattice depth, and this is in agreement with our result as well as with the result of Krämer *et al.* [16]. While we do not predict dependence on the lattice depth, we do predict dependence on the modulation of the excitation along the z axis. In particular, we expect changes in the eigenfrequency if the sites are out of phase with each other, and these changes can be large for typical experimental parameters. So far, such phenomena have not been probed experimentally.

The paper is organized as follows. In Sec. II, we derive the theory used in this paper. In Sec. III, we apply this theory to a Bose-Einstein condensate without vortices and calculate the dispersion relation of the monopole and quadrupole modes in the presence of a lattice. In Sec. IV, we proceed by repeating similar calculation for the vortex state of the Bose-Einstein condensate. We end with a discussion of our results in Sec. V.

II. GROSS-PITAEVSKII THEORY

Our starting point is a cigar-shaped Bose-Einstein condensate trapped by the potential

$$V(\mathbf{r}) = \frac{M}{2}(\omega_r^2 r^2 + \omega_z^2 z^2), \tag{1}$$

where ω_r and ω_z are the radial and axial trapping frequencies, respectively, and M is the atomic mass. As we assume a cigar-shaped trap, we further have that $\omega_z \ll \omega_r$. The condensate also experiences a one-dimensional optical lattice,

$$V_0(\mathbf{r}) = V_0 \sin^2\left(\frac{2\pi z}{\lambda}\right), \tag{2}$$

where V_0 is the lattice depth and λ is the wavelength of the laser light. We assume that the lattice is deep enough so that it dominates over the magnetic trapping potential in the z direction. When this is true and the number of lattice sites is large, i.e., $\lambda \ll l_z = \sqrt{\hbar/M\omega_z}$, we can, in first instance, ignore the magnetic trapping potential in the z direction.

The lattice potential splits the condensate into N_s two-dimensional (quasi)condensates with a two-dimensional droplet shape. We assume that the lattice is sufficiently deep such that its depth is larger than the chemical potential of the two-dimensional (quasi)condensate [21]. Using a Thomas-Fermi approximation for the two-dimensional (quasi)condensates, we obtain a lower boundary that can be expressed as

$$V_0 \gg 2^{9/7}\left[Na\left(\frac{M\omega_r}{\hbar\lambda^2}\right)^{1/4}\right]^{4/7}\hbar\omega_r, \tag{3}$$

where N is the number of atoms per site and a is the three-dimensional scattering length. As a numerical example, we take a ^{87}Rb condensate in a trap with a radial trapping frequency $\omega_r/2\pi = 100$ Hz and a laser-light wavelength of $\lambda = 800$ nm. When the atom number in each site is between 100 and 1000, the lower bound on the trap depth V_0 is between $0.05E_r$ and $0.19E_r$, where $E_r = \hbar^2(2\pi/\lambda)^2/2M$ is the recoil energy of an atom that absorbed one photon from the laser beam.

Although we are interested in a deep lattice, we consider here only the case that there is still full coherence across the condensate array. Specifically, this means that the lattice potential should not be so deep as to induce a Mott-insulator transition. Typically, the required lattice depth to reach the Mott-insulator transition in a three-dimensional lattice with a filling factor of 1 is of the order of $10E_r$. In a one-dimensional lattice, the number of atoms in each lattice site is typically much larger than in a three-dimensional lattice and the transition into the insulating state requires a much deeper lattice. In mean-field theory the Mott-insulator transition in such a system occurs when $U_R > 8NJ$ [22], where U_R and J are, respectively, the characteristic renormalized interaction and hopping parameters of the effective single-mode Bose-Hubbard model with Hamiltonian

$$\hat{H} = -J\sum_{\langle i,j\rangle}\hat{b}_j^\dagger\hat{b}_i + \frac{U_R}{2}\sum_i \hat{n}_i(\hat{n}_i - 1). \tag{4}$$

Using the same numerical values as in the previous paragraph, we estimate the critical lattice depth for the Mott-insulator transition to be between $56E_r$ and $82E_r$, when the number of atoms in each site is again between 100 and 1000. To the best of our knowledge, the Mott-insulator transition in a one-dimensional optical lattice has not yet been observed.

We use trap units from now on, i.e., the unit of energy is $\hbar\omega_r$, the unit of time is $1/\omega_r$, and the unit of length is $l_r = \sqrt{\hbar/M\omega_r}$. The Gross-Pitaevskii energy functional, which describes the system at low temperatures, is then

$$E[\Psi^*,\Psi] = \int d\mathbf{r}\left\{-\frac{1}{2}\Psi^*(\mathbf{r})\nabla^2\Psi(\mathbf{r}) + \left[\frac{1}{2}(x^2+y^2) + \frac{V_0(\mathbf{r})}{\hbar\omega_r} + \frac{T^{2B}}{2}|\Psi(\mathbf{r})|^2\right]|\Psi(\mathbf{r})|^2\right\}, \tag{5}$$

where T^{2B} is the two-body T matrix. In the above units the latter is related to the three-dimensional s-wave scattering length a through $T^{2B}=4\pi a/l_r$.

For a deep lattice potential it is natural to expand the condensate wave function in terms of wave functions that are well localized in the sites. More precisely, we expand

$$\Psi(\mathbf{r})=\sum_n w(z-z_n)\Phi_n(x,y), \tag{6}$$

where n labels the lattice sites and $z_n=\lambda n/2l_r$ is the position of the nth site. For now we do not specify the wave functions $\Phi_n(x,y)$ of the two-dimensional (quasi)condensates, but for the wave function in the z direction, $w(z)$, we use the ground-state wave function of the harmonic approximation to the lattice potential near the lattice minimum. This harmonic trap has the frequency

$$\omega_L=\frac{2\pi}{\lambda}\sqrt{2V_0/M}, \tag{7}$$

and the wave function $w(z)$ is thus given by

$$w(z)=\frac{1}{\pi^{1/4}\sqrt{l_L}}\exp\left(-\frac{z^2}{2l_L^2}\right), \tag{8}$$

where $l_L=\sqrt{\hbar/M\omega_L}$.

Substituting the above ansatz into the energy functional and ignoring all but the nearest-neighbor interactions, we get the energy functional

$$E[\Phi^*,\Phi]=\sum_n\int d^2r\left\{-\frac{1}{2}\Phi_n^*(x,y)\nabla^2\Phi_n(x,y)+\left[\frac{1}{2}(x^2+y^2)+\frac{U_{2D}}{2}|\Phi_n(x,y)|^2\right]|\Phi_n(x,y)|^2-J\sum_{\langle n,m\rangle}\int d^2r\Phi_m^*(x,y)\Phi_n(x,y)\right\}, \tag{9}$$

where $\langle n,m\rangle$ indicates nearest neighbors, and

$$U_{2D}=T^{2B}\int dz|w(z)|^4=4\sqrt{\frac{\pi}{2}}\left(\frac{a}{l_L}\right) \tag{10}$$

is the two-dimensional coupling strength. Moreover, J is the strength of the Josephson coupling between neighboring sites, and we have

$$J=-\int dz w^*(z)\left[-\frac{1}{2}\frac{\partial^2}{\partial z^2}+\frac{V_0(z)}{\hbar\omega_r}\right]w(z+\lambda/2l_r). \tag{11}$$

With these assumptions, J is a time-independent experimentally defined parameter. Approximating the lattice potential near its maximum by an upside-down parabolic potential we can calculate the Gaussian integral, with the result

$$J=\frac{1}{8\pi^2}\left(\frac{\omega_L}{\omega_r}\right)^2\left(\frac{\lambda}{l_r}\right)^2\left[\frac{\pi^2}{4}-1\right]e^{-(\lambda/4l_L)^2}. \tag{12}$$

The energy functional in Eq. (9) is now almost two dimensional. The third dimension is visible only in the last term that describes the coupling between neighboring layers. The energy is characterized by two parameters U_{2D} and J, both of which are experimentally tunable. The importance of the on-site interaction term proportional to U_{2D} can be enhanced by increasing the number of particles in the sites or by making the lattice deeper. Deepening the lattice also decreases the strength of the Josephson coupling J and makes the sites more independent. It should be noted that while J is tunable, it is always positive. Physically, this means that there is always an energetic penalty for having a phase difference between sites.

III. EXCITATIONS OF THE CONDENSATE GROUND STATE

In this section we study the transverse excitations of the ground state of the stack of two-dimensional (quasi)condensates. Using a Gaussian ansatz for the wave functions of the (quasi)condensates, we solve the dispersion relations for the monopole and the quadrupole modes analytically. In Sec. III A we introduce the Gaussian ansatz and solve the excitations for an individial two-dimensional (quasi)condensate. In Sec. III B we proceed to calculate the band structure of the monopole and quadrupole modes in the optical lattice. These sections also include technical details about the calculations. Such details are not repeated in Sec. IV where we consider the vortex state.

A. Excitations for a single two-dimensional (quasi)condensate

To account for the monopole and quadrupole modes of the two-dimensional (quasi)condensates in every site, we use a general Gaussian ansatz for the wave functions, i.e.,

$$\Phi_n(x,y,t)=C_n(t)\exp\left[-\frac{1}{2}[B_{xx,n}(t)x^2+B_{yy,n}(t)y^2+2B_{xy,n}(t)xy]\right]. \tag{13}$$

All three variational parameters $B_{ij,n}(t)\equiv B'_{ij,n}(t)+iB''_{ij,n}(t)$ are complex. From now on, we always use a prime to denote the real part of a complex quantity and a double prime to denote its imaginary part. The wave functions are normalized to the number of particles N at the site, and therefore

$$C_n(t)=\sqrt{\frac{N}{\pi}}[B'_{xx,n}(t)B'_{yy,n}(t)-B'_{xy,n}(t)^2]^{1/4}. \tag{14}$$

As we fix the number of particles in every site, we are excluding the Bogoliubov modes propagating along the z axis. It is, however, not difficult to account also for these modes as

we show later on. The equations of motion for the variational parameters can be derived from the Lagrangian

$$L[\Phi^*,\Phi]=\frac{i}{2}\int d^2r\left(\sum_n \Phi_n^*(x,y,t)\frac{\partial\Phi_n(x,y,t)}{\partial t}-\Phi_n(x,y,t)\frac{\partial\Phi_n^*(x,y,t)}{\partial t}\right)-E[\Phi^*,\Phi]. \tag{15}$$

Let us first investigate the behavior of an individual two-dimensional (quasi)condensate. Without the interlayer coupling, the part of the Lagrangian quadratic in the deviations $\epsilon_{ij}(t)$ turns out to be equal to

$$\begin{aligned}\frac{L}{N}=&-\frac{1}{4B_0^2}(\epsilon'_{xx}\dot{\epsilon}''_{xx}+\epsilon'_{yy}\dot{\epsilon}''_{yy}+2\epsilon'_{xy}\dot{\epsilon}''_{xy})+\frac{U}{B_0}\left[\frac{(\epsilon'_{xx}-\epsilon'_{yy})^2}{8}+\frac{\epsilon'^2_{xy}}{2}\right]+-\left(\frac{1}{2B_0^3}+\frac{1}{2B_0}\right)(\epsilon'^2_{xx}+\epsilon'^2_{yy}+\epsilon'_{xx}\epsilon'_{yy}+\epsilon'^2_{xy})\\&+\left(\frac{1}{4B_0^3}+\frac{3}{4B_0}\right)(\epsilon'_{xx}+\epsilon'_{yy})^2-\frac{1}{4B_0}[(\epsilon'_{xx}+\epsilon'_{yy})^2+2\epsilon'_{xx}\epsilon'_{yy}+\epsilon''^2_{xx}+\epsilon''^2_{yy}+2\epsilon''^2_{xy}],\end{aligned} \tag{16}$$

where

$$U=\frac{N}{\sqrt{2\pi}}\left(\frac{a}{l_r}\right)\sqrt{\frac{\omega_L}{\omega_r}}. \tag{17}$$

We also defined the equilibrium solution of $B_{ii}(t)$ as B_0. Hence, $B_{ij}(t)=B_0\delta_{ij}+\epsilon_{ij}(t)$. We also suppressed the site index n. The equilibrium solution B_0 is given by minimizing the zeroth-order term of the energy, i.e.,

$$E_0=\frac{1}{2B_0}+\frac{B_0}{2}+UB_0, \tag{18}$$

with the result

$$B_0=\sqrt{\frac{1}{1+2U}}. \tag{19}$$

In Eq. (16) we show only the part relevant for the dynamics and we ignored the zeroth-order term, whose minimization leads to the result in Eq. (19).

We are now in a position to find the frequencies for the collective excitations we are interested in. Let us start with the monopole $m=0$ mode, which is alternatively also called the breathing mode. For the monopole mode we can set $\epsilon_{xx}=\epsilon_{yy}=\epsilon$ and $\epsilon_{xy}=0$. With this choice the Lagrangian is greatly simplified to

$$\frac{L}{N}=-\frac{1}{2B_0^2}\left[\epsilon'\dot{\epsilon}''-\frac{1}{B_0}\epsilon'^2-B_0\epsilon''^2\right]. \tag{20}$$

The equations of motion for ϵ' and ϵ'' are the Euler-Lagrange equations that result in two first-order differential equations,

$$\begin{aligned}&\dot{\epsilon}'+2B_0\epsilon''=0,\\&-\dot{\epsilon}''+\frac{2}{B_0}\epsilon'=0.\end{aligned} \tag{21}$$

These equations can be cast into a single second-order differential equation for ϵ',

$$\ddot{\epsilon}'=-4\epsilon', \tag{22}$$

which describes sinusoidal oscillation with a frequency of 2. The frequency of the monopole mode is therefore

$$\omega_0=2, \tag{23}$$

and it is independent of the strength of interactions. This is in agreement with previous results [23].

The quadrupole $m=\pm2$ modes are captured by the choice $\epsilon_{xx}=-\epsilon_{yy}=\epsilon$. We then have just two (complex) variational parameters, ϵ and ϵ_{xy}. In the Lagrangian in Eq. (16) there are no terms that couple ϵ to ϵ_{xy}. Therefore, the dynamics of these parameters separates, and both turn out to have the same oscillation frequency. Above we gave the necessary technical details in the derivation of the monopole-mode frequency. As the quadrupole-mode frequency can be dealt with in a similar fashion, we simply give the result. The quadrupole-mode frequencies are given by

$$\omega_{\pm2}=\sqrt{2+2B_0^2}. \tag{24}$$

For the ideal gas, $B_0=1$ and the quadrupole frequency is again 2. In the Thomas-Fermi limit, B_0 tends to zero and the quadrupole frequencies approach $\omega_{\pm2}\to\sqrt{2}$. Again, this result is as expected [17,24,25]. Our treatment also captures the scissors mode [26], but in the axial symmetric case we are considering here, the scissors mode turns out to be degenerate with the quadrupole mode.

Incidentally, it should be remembered that the degeneracy of the quadrupole modes is lifted in a rotating trap. If the trap is rotating with frequency Ω around the z axis, we should include a term $-\Omega\langle L_z\rangle$ into the energy functional, where $\langle L_z\rangle$ is the expectation value of the angular-momentum component in the z direction. The angular momentum of the equilibrium solution is zero and the new term will only contribute in second order. The new contribution to the energy is

$$-\Omega\langle L_z\rangle=\frac{\Omega}{B_0^2}[\epsilon'_{xy}\epsilon''-\epsilon''_{xy}\epsilon']. \tag{25}$$

This term couples the dynamics of ϵ and ϵ_{xy}, but the resulting 2×2 matrix problem is easy to solve. The quadrupole-mode frequencies in a rotating trap are

$$\omega_{\pm2}=\sqrt{2}[(1+B_0^2)^{1/2}\pm\sqrt{2}\Omega]. \tag{26}$$

From this result it is clear that the quadrupole mode with $m=-2$ becomes thermodynamically unstable when $\Omega > \sqrt{(1+B_0^2)/2}$. This result corresponds to the Landau criterion for the quadrupole modes, and has been shown to play an important role in the nucleation of vortices [27–31].

B. Influence of the lattice on the excitation frequencies

We are now in the position to discuss the influence of the lattice potential. To make progress we must determine the coupling integral

$$I_{mn}=\int d^2r\Phi_m^*(x,y)\Phi_n(x,y) \tag{27}$$

to a sufficient accuracy. This will contribute to the energy a Josephson coupling

$$H_J=-J\sum_{\langle n,m\rangle} I'_{mn}, \tag{28}$$

where the $\langle n,m\rangle$ indicates nearest neighbors. Here the imaginary part of I_{mn} is not relevant since its contribution to the energy vanishes when the sum over the nearest-neighbors is calculated. For the monopole mode we get, up to second order in the deviations, the result

$$\frac{I'_{mn}}{N}=1-\frac{1}{8B_0^2}(\epsilon_n'^2+\epsilon_m'^2+2\epsilon_n''^2+2\epsilon_m''^2)+\frac{1}{4B_0^2}\epsilon_n'\epsilon_m' + \frac{1}{2B_0^2}\epsilon_n''\epsilon_m'', \tag{29}$$

and for the quadrupole mode we have

$$\frac{I'_{mn}}{N}=1-\frac{1}{8B_0^2}(|\epsilon_n|^2+|\epsilon_m|^2+|\epsilon_{xy,n}|^2+|\epsilon_{xy,m}|^2) + \frac{1}{4B_0^2}(\epsilon_n'\epsilon_m'+\epsilon_n''\epsilon_m''+\epsilon_{xy,n}'\epsilon_{xy,m}'+\epsilon_{xy,n}''\epsilon_{xy,m}''). \tag{30}$$

In these formulas the first subindex of $\epsilon_{xy,n}$ identifies the variational parameter in question and the second one indicates the lattice site. For identical nearest-neighbor wave functions the overlap integral I_{mn} should be exactly N, which is indeed the case in both Eqs. (29) and (30).

Some terms in Eqs. (29) and (30) are purely on site, but terms of the type $\epsilon_n\epsilon_m$ are not. This complication is remedied by going to Fourier space. We define the Fourier transform in such a way that the function f_n in coordinate space is expressed in terms of its transform f_k as

$$f_n=\frac{1}{\sqrt{N_s}}\sum_{k=-(2\pi/\lambda)[1-(1/N_s)]}^{(2\pi/\lambda)[1-(1/N_s)]}\exp[ikz_n]f_k. \tag{31}$$

Here N_s is the number of lattice sites which we, for notational convenience, assume to be an odd number. Moreover, k is the wave number and the lattice spacing is $d=\lambda/2$.

First we transform the diagonal terms in the Lagrangian. For example,

$$\sum_n f_n^2=\sum_n\frac{1}{N_s}\sum_{k,k'}f_kf_{k'}\exp[iz_n(k+k')] =\sum_k f_kf_{-k} =\sum_k |f_k|^2, \tag{32}$$

where the sum over the lattice sites n gave the Kronecker delta $\delta_{k',-k}$ which removed one of the momentum sums. The last step is a result of the fact that f_n was a real function, so $f_k^*=f_{-k}$. Nearest-neighbor terms are somewhat more complicated. As an example,

$$\sum_{\langle n,m\rangle} f_nf_m=\frac{1}{2N_s}\sum_n\sum_{k,k'}f_kf_{k'}\{\exp[i(kz_n+k'z_{n+1})] +\exp[i(kz_n+k'z_{n-1})]\}. \tag{33}$$

We can perform the sum over n and get

$$\sum_{\langle n,m\rangle} f_nf_m=\sum_{k,k'}\cos(k'\lambda/2)f_kf_{k'}\delta_{k',-k}=\sum_k\cos(k\lambda/2)|f_k|^2. \tag{34}$$

In Fourier space the Josephson coupling H_J generally thus introduces factors of $\cos(k\lambda/2)-1$ into the Lagrangian.

Now that we know how to transform to Fourier space, we can proceed to derive equations of motion for each value of the wave vector k. Since two different values of the wave vectors do not couple, this is not technically any more complicated than our previous treatment of an individual (quasi)-condensate. The equations for each wave vector can be solved separately. We demonstrate this again for the simplest case, namely, the breathing mode. Let the Fourier transform of ϵ_n be ϵ_k. In Fourier space the Lagrangian for the breathing mode is

$$L=-\frac{1}{2B_0^2}\left\{\sum_k \epsilon_k'^*\dot{\epsilon}_k''+\left\{\frac{1}{B_0}-J\left[\cos\left(\frac{k\lambda}{2}\right)-1\right]\right\}|\epsilon_k'|^2 +\left[B_0-2J\left(\cos\left(\frac{k\lambda}{2}\right)-1\right)\right]|\epsilon_k''|^2\right\}. \tag{35}$$

Keeping in mind that $\epsilon_{-k}=\epsilon_k^*$, we get equations of motion for ϵ_k' and ϵ_k''. For example, by considering the variation of the Lagrangian with respect to ϵ''_{-k} we get

$$\dot{\epsilon}_k'-2\left\{B_0-2J\left[\cos\left(\frac{k\lambda}{2}\right)-1\right]\right\}\epsilon_k''=0, \tag{36}$$

and by considering variations with respect to ϵ'_{-k} we get the differential equation for ϵ''_k,

$$\dot{\epsilon}''_k + 2\left\{\frac{1}{B_0} - J\left[\cos\left(\frac{k\lambda}{2}\right) - 1\right]\right\}\epsilon'_k = 0. \tag{37}$$

The dispersion relation for the monopole mode can now be simply read out from this pair of equations. The quadrupole modes can be dealt with in the same way although the equations are somewhat longer.

For convenience we assume that the contribution from terms proportional to J^2 are very small. With this simplification we get the dispersion relations for the monopole and quadrupole modes,

$$\omega_0(k) = 2\left\{1 - J\left(B_0 + \frac{2}{B_0}\right)\left[\cos\left(\frac{k\lambda}{2}\right) - 1\right]\right\}^{1/2}, \tag{38}$$

$$\omega_{\pm 2}(k) = \sqrt{2}\left\{1 + B_0^2 - J\left(3B_0 + \frac{1}{B_0}\right)\left[\cos\left(\frac{k\lambda}{2}\right) - 1\right]\right\}^{1/2}. \tag{39}$$

We emphasize that our results where terms under the square root proportional to J^2 are ignored should be used with some caution. The terms proportional to J^2 are not always negligible compared to the other contributions. In particular, if the trap depth or the on-site number of particles is small, there is a range of experimentally relevant parameter values where terms proportional to J^2 can be relatively large and should be included. They will not change the qualitative behavior of the dispersion relations, but can affect quantitative results. While we choose to work in the regime where terms proportional to J^2 are small, it is not difficult to include these missing terms. For example, Eqs. (36) and (37) show that the exact frequency for the monopole mode obeys

$$\omega_0^2(k) = 4\left\{B_0 - 2J\left[\cos\left(\frac{k\lambda}{2}\right) - 1\right]\right\}\left\{\frac{1}{B_0} - J\left[\cos\left(\frac{k\lambda}{2}\right) - 1\right]\right\}. \tag{40}$$

In Fig. 1 we show the dispersion relation for the monopole mode as a function of k and U.

In the limit of long wavelengths, it is permissible to expand the cosine factors. The excitation has then the same dispersion as that of a free-particle $\Delta + \hbar^2 k^2/2m^*$ with some effective mass m^* and a gap Δ. For the monopole mode we, therefore, predict an effective mass

$$m_0^* = \frac{4B_0}{J(B_0^2+2)}\left(\frac{\hbar}{\omega_r \lambda^2}\right), \tag{41}$$

and for the quadrupole mode we get

$$m_{\pm 2}^* = \frac{4B_0\sqrt{2}}{J(3B_0^2+1)}\left(\frac{\hbar}{\omega_r \lambda^2}\right). \tag{42}$$

It is quite interesting to observe that the effective masses of different modes are different. In particular, the effective mass of the quadrupole mode is bigger than the effective mass of the monopole mode. This can be understood by considering the overlap integral between neighboring sites. For the monopole mode the coupling between the nearest neighbors is, to a large extent, determined by the integral

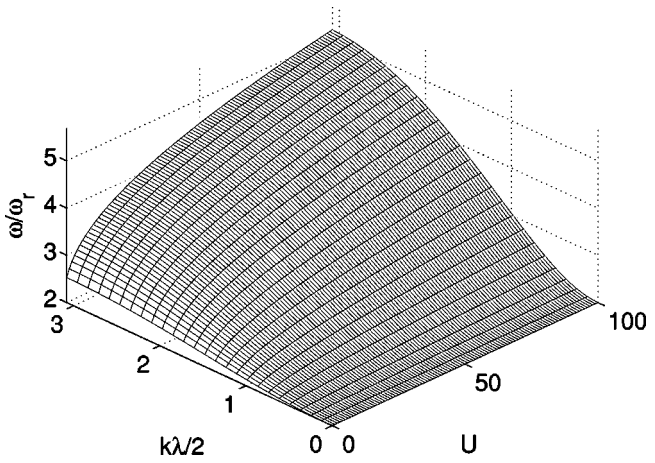

FIG. 1. Monopole-mode frequency as a function of k and U, when $J = 0.05$. The surface in this figure was calculated using Eq. (38).

$$\int d^2r |\Phi_0(x,y)|^2 (x^2+y^2)^2,$$

where $\Phi_0(x,y)$ is the equilibrium wave function. In contrast, for the quadrupole mode the coupling is determined by the integral

$$\int d^2r |\Phi_0(x,y)|^2 (x^2-y^2)^2.$$

It is clear that the latter integral is smaller than the first one. As the effective mass is inversily proportional to the strength of the nearest-neighbor coupling, the quadrupole mode therefore has a bigger effective mass.

The fact that the dispersion relation is similar to the free-particle dispersion relation is reflected in the dynamics. A sinusoidal modulation moves with velocity $v \simeq \hbar\langle k\rangle/m^*$ in the z direction. In a finite system a pure sinusoidal modulation is not possible and the excitation corresponds to a wave packet centered around $\langle k\rangle$ and with some nonzero width Δk. If the system is large enough, i.e., much bigger than $2\pi/\Delta k$, the width of the packet can be small and one should be able to observe such propagation before the excitation hits the outer edge of the condensate.

More generally, we can expand the dispersion relation around any value of the wave vector. In terms of a function $C(J,B_0)$ that depends on the mode in question, the excitation energy up to lowest order in J looks like

$$\omega(k) = \omega(0) + C(J,B_0)\left[\cos\left(\frac{k\lambda}{2}\right) - 1\right]. \tag{43}$$

Expanding this expression around k_0, we get

$$\omega(k)\approx\omega(k_0)-C(J,B_0)\left[\frac{\lambda}{2}\sin\left(\frac{k_0\lambda}{2}\right)(k-k_0)+\frac{\lambda^2}{8}\cos\left(\frac{k_0\lambda}{2}\right)(k-k_0)^2\right]. \quad (44)$$

When $k_0=0$ we get the results for the effective masses we presented earlier, but some special cases are also of interest. In particular, when $k\lambda/2=\pi$, we obtain the same expansion as with $k=0$, but the constant in front of $(k-k_0)^2$ has a negative sign. In this regime the effective mass is therefore negative. In the regime of a negative effective mass one encounters modulational instabilities as discussed in Refs. [11–13].

IV. EXCITATIONS OF THE VORTEX STATE

In this section we consider a system of weakly coupled two-dimensional (quasi)condensates, which has a vortex piercing through the center of each (quasi)condensate. For such a system our earlier ansatz in Eq. (13) is inadequate. For an individual condensate it is known that the presence of a vortex should not change the dispersion of the monopole mode, but it will lift the degeneracy of the quadrupole modes. Physically, this is due to the fact that the quadrupole excitation, depending on the sign of the quantum number m, travels either in the same direction of the superfluid flow or opposite to it. As the monopole mode is easier to tackle than the quadrupole modes, we start with that in Sec. IV A. In Sec. IV B we solve for the quadrupole modes of an individual two-dimensional (quasi)condensate and in Sec. IV C we include also for the quadrupole mode the optical lattice into our discussion.

A. Monopole mode in the presence of a vortex

The vortex state has a superfluid flow around the vortex core. This flow diverges in the core, and for this reason the density of the condensate must vanish in the vortex core. The simplest ansatz having these two desired properties is (in polar coordinates)

$$\Phi_n(r,\phi)\propto r\exp[i\phi]\exp\left[-\frac{B_0r^2}{2}\right]\exp\left[-\frac{\epsilon_n(t)r^2}{2}\right]. \quad (45)$$

The ansatz is almost the same as in the preceding section for the monopole mode of the state without a vortex. The only differences are the first two factors that give the vortex the properties we were after. The size of the vortex core region in Eq. (45) is about $1/\sqrt{B_0}$ and it does not diminish as the number of particles is increased. This is in principle incorrect, since the length scale for the vortex core size is set by the coherence length, and the coherence length in the center of the condensate gets smaller as the number of particles is increased. We expect that this unphysical behavior close to the vortex core is not relevant to the physics of the collective modes at hand. In the end of the calculations we can reproduce the known results for the individual two-dimensional droplet to a good accuracy, and thus our expectations are indeed well justified.

Using similar techniques as for the condensate without a vortex, we calculate the monopole mode of a condensate with a vortex as

$$\omega_0(k)=2\left\{1-3J\left(B_0+\frac{1}{B_0}\right)\left[\cos\left(\frac{k\lambda}{2}\right)-1\right]\right\}^{1/2}, \quad (46)$$

where we have again assumed that J^2 terms under the square root can be ignored. The equilibrium solution is now given by

$$B_0=\sqrt{\frac{2}{2+U}}. \quad (47)$$

The result is similar to Eq. (38), but the constant in front of the cosine term is different indicating a difference in the effective mass. For the monopole mode in the presence of a vortex, we get

$$m^*_{0,v}=\frac{4B_0}{3J(B_0^2+1)}\left(\frac{\hbar}{\omega_r\lambda^2}\right). \quad (48)$$

We can see that the effective mass of the monopole mode of the vortex state is somewhat smaller than the effective mass in the absence of a vortex. This can be understood by comparing the relevant overlap integrals for the wave functions with and without the vortex. Since the (quasi)condensate wave function with a vortex is more extended than without a vortex, the strength of the nearest-neighbor coupling is increased and, therefore, the effective mass is reduced.

B. Quadrupole modes of the single two-dimensional droplet in the presence of a vortex

As we mentioned before the quadrupole modes are more complicated. For the quadrupole modes, we use the ansatz

$$\begin{aligned}\Phi_n(r,\phi)&\propto r\exp[i\phi]\exp\left[-\frac{B_0r^2}{2}\right]\\&\quad\times\exp\left[-\epsilon\frac{(x^2-y^2)}{2}-\epsilon_{xy}xy\right][1+\alpha\exp[-2i\phi]]\\&\simeq r\exp[i\phi]\exp\left[-\frac{B_0r^2}{2}\right]\left[1+\cos(2\phi)\left(\alpha-\frac{\epsilon}{2}r^2\right)\right.\\&\quad\left.-\sin(2\phi)\left(i\alpha+\frac{\epsilon_{xy}}{2}r^2\right)\right], \quad (49)\end{aligned}$$

where α denotes a new variational parameter and the last expression is an expansion of the first line to the first order in the deviations. This ansatz looks somewhat complicated, but this is needed to build in the relevant physics. This is most easily seen by considering the noninteracting limit where the wave functions are known analytically.

In the noninteracting limit the vortex states with angular-momentum projections equal to $\pm N$ are degenerate. This implies that linear superpositions of these states have the same energy. As a result, there exists a quadrupole mode with zero frequency in this limit. To capture this mode, the

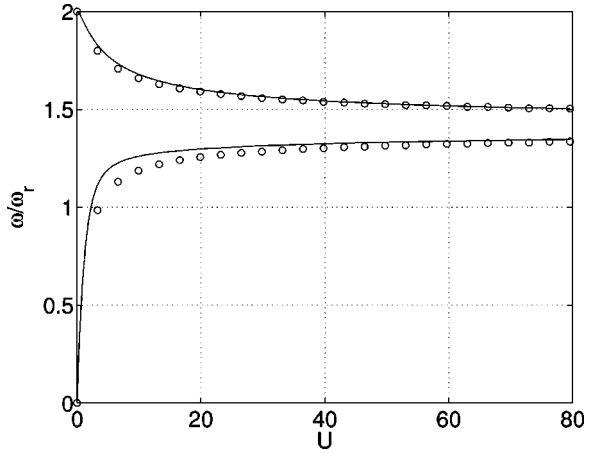

FIG. 2. Splitting of the quadrupole modes for the Bose-Einstein condensate with a vortex as a function of the interaction strength. The solid line is the analytical result based on the ansatz in Eq. (49) and the open circles are calculated by solving the Bogoliubov–de Gennes equations numerically.

variational parameter α is included in the ansatz. To understand this, assume that $\alpha=0$ and expand the exponent in Eq. (49). We get

$$\exp\left[-\epsilon\frac{(x^2-y^2)}{2}-\epsilon_{xy}xy\right] = 1-\frac{\epsilon r^2}{2}\cos(2\phi)-\frac{\epsilon_{xy}r^2}{2}\sin(2\phi)+\mathcal{O}(\epsilon^2,\epsilon_{xy}^2,\epsilon\epsilon_{xy}). \tag{50}$$

For clarity, assume also that ϵ is real and $\epsilon_{xy}=-i\epsilon$. The disturbance then couples to the wave function

$$r\exp[i\phi]\exp\left[-\frac{B_0 r^2}{2}\right]r^2\exp[-2i\phi],$$

which is the wave function of the antivortex state multiplied by r^2. This state has obviously a different energy than the true antivortex wave function. As a result, the ansatz without α gives a wrong frequency for this mode in the ideal-gas limit. To avoid this problem we need the additional variational parameter α to give a nonvanishing amplitude for the correct antivortex wave function in the ideal gas limit. The fact that this ansatz really couples to the correct antivortex wave function is most clearly seen by setting $\epsilon=\epsilon_{xy}=0$ in Eq. (49). Otherwise, the ansatz is very similar to the ansatz we used for the (quasi)condensate without the vortex. In the noninteracting limit the $m=+2$ mode requires coupling to a wave function with angular momentum $m=3$ and with a small distance behavior that should be proportional to r^3. In Eq. (49) this is indeed the case, as can be verified by setting α equal to 0.

Using the above ansatz we can determine the quadrupole modes of a single two-dimensional droplet analytically for the full parameter regime from the noninteracting limit to the Thomas-Fermi regime. The equilibrium solution is the same as for the monopole mode and is given by Eq. (47). To second order in the deviations, the various contributions to the Lagrangian are

$$L_T=-2\alpha'\dot{\alpha}''-\frac{3}{2B_0^2}(\epsilon'\dot{\epsilon}''+\epsilon_{xy}'\dot{\epsilon}_{xy}'') +\frac{1}{B_0}[\alpha'(\dot{\epsilon}''+\dot{\epsilon}_{xy}')+\alpha''(\dot{\epsilon}_{xy}''-\dot{\epsilon}')],$$

$$L_V=\frac{3}{4B_0^3}(|\epsilon|^2+|\epsilon_{xy}|^2)-\frac{1}{2B_0}[\alpha'(\epsilon'-\epsilon_{xy}'')+\alpha''(\epsilon''+\epsilon_{xy}')],$$

$$L_K=\frac{1}{4B_0}(|\epsilon|^2+|\epsilon_{xy}|^2+4\epsilon_r\epsilon_{xy}''-4\epsilon''\epsilon_{xy}') +\frac{1}{2}[\alpha'(\epsilon'-\epsilon_{xy}'')+\alpha''(\epsilon''+\epsilon_{xy}')],$$

$$L_{NL}=UB_0\left\{|\alpha|^2+\frac{3}{8B_0^2}(\epsilon'^2-\epsilon''^2+\epsilon_{xy}'^2-\epsilon_{xy}''^2) -\frac{1}{4B_0}[\alpha'(5\epsilon'+\epsilon_{xy}'')+\alpha''(5\epsilon_{xy}'-\epsilon'')]\right\}, \tag{51}$$

where L_T is due to the part of the Lagrangian containing the time derivatives, L_V is due to the potential energy, L_K is due to the kinetic energy, and L_{NL} is the contribution due to the interactions between atoms.

With this result we can solve for the eigenmodes of the system. The problem is essentially that of solving the eigenvalues of a 3×3 matrix. This matrix has three (generally) nondegenerate eigenvalues and two of these correspond to the quadrupole modes. The third mode is of no interest to us here. In this modes the deviation from the equilibrium is a superposition of various trap states, among which the $m=5$ component has an incorrect short distance behavior that causes the energy of this mode to strongly increase with increasing atom number. The frequencies of the quadrupole modes can be calculated analytically, but the results are too long to be given here. However, they do not cause any computational problems. In Fig. 2 we show the frequencies of the quadrupole modes based on our ansatz and compare them against the values computed numerically with the Bogoliubov–de Gennes equations [32]. The agreement is very good over the whole range of interaction strengths.

In the limit of a nearly ideal gas, the quadrupole frequencies are $\omega_{-2}=U$ and $\omega_2=2$. For large atom numbers the quadrupole-mode frequencies are given by

$$\omega_{\pm2}=\sqrt{2}\pm\frac{1}{\sqrt{2U}}, \tag{52}$$

and the splitting between the modes is $\omega_2-\omega_{-2}=\sqrt{2/U}$. Zambelli and Stringari [33] used sum rules to show that the splitting between the quadrupole modes in the limit of large atom numbers should be

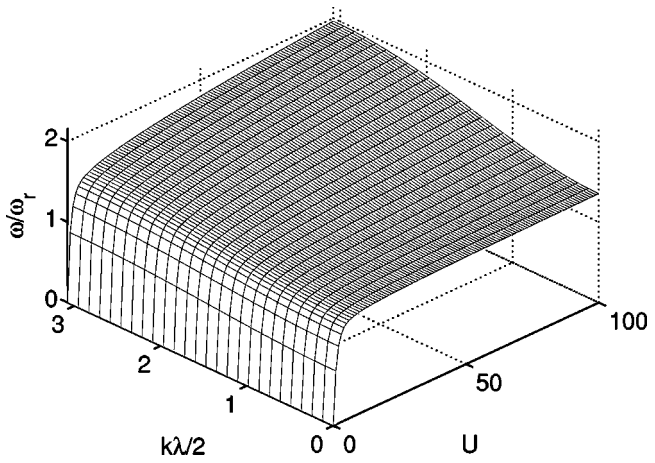

FIG. 3. Dispersion of the quadrupole mode with $m=-2$ for the Bose-Einstein condensate with a vortex when $J=0.05$. The figure is based on the wave-function ansatz in Eq. (49).

$$\omega_2-\omega_{-2}=\frac{2\langle L_z\rangle}{\langle r^2\rangle}. \tag{53}$$

Here L_z is the z component of the angular-momentum operator. With our ansatz we have $\langle L_z\rangle=1$ and $\langle r^2\rangle=2/B_0$, and the splitting of the quadrupole modes is indeed the same as the result based on the sum-rule approach.

C. Influence of the lattice on the quadrupole modes of the vortex state

Including the lattice structure makes the already complicated equations even more complicated [34]. In Fourier space the nearest-neighbor interaction introduces a new term to the Hamiltonian,

$$H_J=-J\sum_k\left[\cos\left(\frac{k\lambda}{2}\right)-1\right]\left\{2|\alpha_k|^2+\frac{3}{2B_0^2}(|\epsilon_k|^2+|\epsilon_{xy,k}|^2)\right.$$
$$\left.+\frac{2}{B_0}[\alpha_k'(\epsilon_{xy,k}''-\epsilon_k')-\alpha_k''(\epsilon_k''+\epsilon_{xy,k}')]\right\}, \tag{54}$$

where α_k' is the Fourier transform of the real part of α_n, ϵ_k' is the Fourier transform of the real part of ϵ, and $\epsilon_{xy,k}'$ is the Fourier-transform of the real part of ϵ_{xy}. Similar notation applies to the imaginary parts and, for example, $|\epsilon_k|^2=\epsilon_k'\epsilon_{-k}'+\epsilon_k''\epsilon_{-k}''$. In Figs. 3 and 4 we show in detail the resulting dispersion relations for the quadrupole modes as a function of k and interaction strength U.

Even though the general formulas are too complictated to be given here, the ideal-gas limit and the Thomas-Fermi limit give us simple formulas. In the limit of weak interactions we have $\omega_{-2}=U-2J[\cos(k\lambda/2)-1]$ and $\omega_2=2-2J[\cos(k\lambda/2)-1]$, and in the limit of strong interactions or large particle numbers we have

$$\omega_{\pm 2,v}=\sqrt{2}\left\{1-\frac{3J}{4}\sqrt{\frac{U}{2}}\left[\cos\left(\frac{k\lambda}{2}\right)-1\right]\right\}. \tag{55}$$

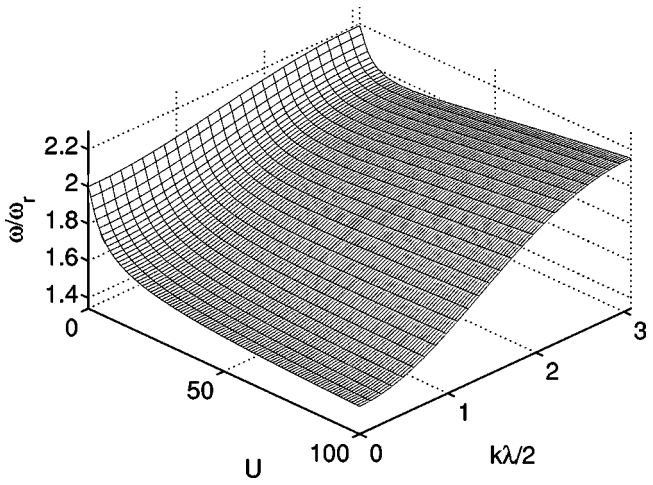

FIG. 4. Dispersion of the quadrupole mode with $m=2$ for the Bose-Einstein condensate with a vortex when $J=0.05$. The figure is based on the wave-function ansatz in Eq. (49). Note that for clarity, the viewing angle is different from the previous figures.

In the limit of large particle numbers the effective mass of the quadrupole modes thus becomes

$$m^*_{\pm 2,v}=\frac{16}{3J\sqrt{U}}\left(\frac{\hbar}{\omega_r\lambda^2}\right). \tag{56}$$

This result indicates that we expect the quadrupole modes to have about three times larger effective mass than the breathing mode. Again, this can be understood by overlap arguments.

V. SUMMARY AND CONCLUSIONS

We have calculated the band structure of the most important transverse collective excitations of a stack of two-dimensional Bose-Einstein condensates in a one-dimensional optical lattice with and without a vortex. Our variational approach enables us to cross over smoothly from the ideal gas into the Thomas-Fermi regime and to treat the interlayer coupling without other approximations that those involved in the variational ansatz. We have also calculated the short-wavelength part of the excitation spectra, which means that in our approach neighboring sites can be completely out of phase with each other. Using our general results for the excitation frequencies, we derived predictions for the effective mass of the monopole and quadrupole modes. We noticed that the effective mass is sensitive to the mode in question as well as to the presence of a vortex. In this paper we have only focused on the linear response of the system. For large modulations, nonlinear effects can become important [11–13]. In particular, assumptions about a nearly homogeneous condensate can break down as the system becomes dynamically unstable towards large density modulations.

Experimentally, the kind of excitations we have discussed in this paper can be created by modulating the radial trapping frequency ω_r as a function of z. One possible way to excite the monopole modes is to have two counterpropagating laser

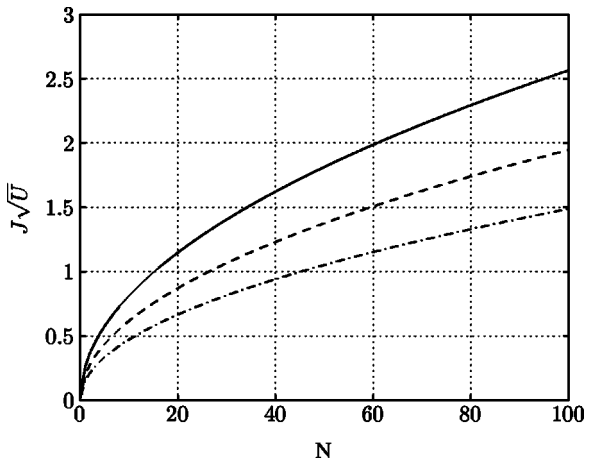

FIG. 5. The quantity $J\sqrt{U}$ as a function of the number of ^{87}Rb atoms in the each lattice site for different lattice depths. The solid line is for the depth $V_0=8E_r$, the dashed line is for $V_0=9E_r$, and the dot dashed line is for $V_0=10E_r$. The wavelength of the laser light was taken to be $\lambda=800$ nm, and the radial trapping frequency was $\omega_r/2\pi=100$ Hz.

beams with a Gaussian intensity profile. Due to the optical dipole force, the intensity profile of each one of the beams would provide the trapping in the radial direction, while the interference between the beams would provide the necessary modulation. To excite equal superposition of $m=\pm 2$ quadrupole modes, sheets of laser light can be considered.

In the limit of large interactions the constant in front of the k-dependent part of the dispersion relations always scales with $J\sqrt{U}$. This number is a good measure of how strong the effects due to the lattice are. If this number is small, the lattice effects are hard to distinguish experimentally from the dominant single-site result. In Fig. 5, we plot $J\sqrt{U}$ as a function of the on-site atom number for a few different lattice depths. As can be seen, the effects of the lattice for the modes we are considering can be very pronounced and should be easily observable.

In the system we have discussed in this paper, each (quasi)condensate becomes very quickly two dimensional as the depth of the lattice is increased. In particular, the coherence length in the center of the two-dimensional (quasi)condensate quickly becomes larger than the thickness of the two-dimensional droplet. In low dimensions phase fluctuations are expected to be more pronounced [35–37]. In our treatment we ignore such fluctuations. In a two-dimensional system there is a true condensate at zero temperature, and then the phase fluctuations are not expected to play a major role. At nonzero temperatures phase fluctuations become more important, but are expected to be more pronounced between sites that are well separated. In our parameter regime the tunneling term coupling neighboring sites will establish phase coherence between neighbors. As a result, the two dimensional (quasi)condensates are not strictly two-dimensional since they ''see'' the third direction through the tunneling term. As the distance between the sites increases, the phases become less correlated, but as we are only interested in the nearest-neighbor couplings, such effects are not important. Consequently, we expect our model to be applicable also at small but nonzero temperatures. Phase fluctuations may cause a slight reduction in the strength of the Josephson coupling, but would leave our results otherwise unchanged.

In this paper we have chosen to fix the number of atoms in every two-dimensional (quasi)condensate. In our variational approach it is not difficult to include atom number as well as global phase fluctuations by replacing in our variational ansatz $\sqrt{N}$ by $\sqrt{N_n(t)}e^{i\nu_n(t)}$, where N_n denotes the number of atoms and ν_n the global phase of the (quasi)condensate in every site. In the simplest case where we neglect the couplings with the transverse modes, we find that at long wavelengths there exists a phonon mode with the sound velocity

$$c_s=\sqrt{\frac{UJ}{\sqrt{1+2U}}\left(\frac{\hbar\omega_r}{m}\right)}\lambda/l_r, \tag{57}$$

which agrees exactly with the results obtained previously [8,16,38].

In a recent experiment the Kelvin modes of a Bose-Einstein condensate with a vortex were observed [10]. In the model that we have presented in this paper the vortex is always in the center of each pancake. In the future we plan to relax this condition and consider also the dynamics of the vortex. In this manner it is possible to study the Kelvin modes in an optical lattice, and in particular their coupling to the transverse excitations, which were our main focus here.

ACKNOWLEDGMENTS

This work was supported by the Stichting voor Fundamenteel Onderzoek der Materie (FOM), which is supported by the Nederlandse Organisatie voor Wetenschaplijk Onderzoek (NWO).

[1] M. Cristiani, O. Morsch, J.H. Müller, D. Ciampini, and E. Arimondo, Phys. Rev. A **65**, 063612 (2002).
[2] Y.B. Ovchinnikov, J.H. Müller, M.R. Doery, E.J.D. Vredenbregt, K. Helmerson, S.L. Rolston, and W.D. Phillips, Phys. Rev. Lett. **83**, 284 (1999).
[3] C. Orzel, A.K. Tuchman, M.L. Fenselau, M. Yasuda, and M.A. Kasevich, Science **291**, 2386 (2001).
[4] M. Greiner, O. Mandel, T.W. Hänsch, and I. Bloch, Nature (London) **419**, 51 (2002).
[5] F.S. Cataliotti, S. Burger, C. Fort, P. Maddaloni, F. Minardi, A. Trombettoni, A. Smerzi, and M. Inguscio, Science **293**, 843 (2001).
[6] S. Burger, F.S. Cataliotti, C. Fort, F. Minardi, M. Inguscio, M.L. Chiofalo, and M.P. Tosi, Phys. Rev. Lett. **86**, 4447 (2001).
[7] D. Jaksch, C. Bruder, J. Cirac, C.W. Gardiner, and P. Zoller,

Phys. Rev. Lett. **81**, 3108 (1998).
[8] D. van Oosten, P. van der Straten, and H.T.C. Stoof, Phys. Rev. A **63**, 053601 (2001).
[9] M. Greiner, O. Mandel, T. Esslinger, T.W. Hänsch, and I. Bloch, Nature (London) **415**, 39 (2002).
[10] V. Bretin, P. Rosenbusch, F. Chevy, G.V. Shlyapnikov, and J. Dalibard, Phys. Rev. Lett. **90**, 100403 (2003).
[11] B. Wu and Q. Niu, Phys. Rev. A **64**, 061603 (2001).
[12] V.V. Konotop and M. Salerno, Phys. Rev. A **65**, 021602 (2002).
[13] B.B. Baizakov, V.V. Konotop, and M. Salerno, J. Phys. B **35**, 5105 (2002).
[14] Y.B. Band and M. Trippenbach, Phys. Rev. A **65**, 053602 (2002).
[15] P. Massignan and M. Modugno, Phys. Rev. A **67**, 023614 (2003).
[16] M. Krämer, L. Pitaevskii, and S. Stringari, Phys. Rev. Lett. **88**, 180404 (2002).
[17] S. Stringari, Phys. Rev. Lett. **77**, 2360 (1996).
[18] M. Greiner, I. Bloch, O. Mandel, T. Hänsch, and T. Esslinger, Appl. Phys. B: Lasers Opt. **B73**, 769 (2001).
[19] O. Morsch, M. Cristiani, J.H. Müller, D. Ciampini, and E. Arimondo, Phys. Rev. A **66**, 021601 (2002).
[20] C. Fort, F.S. Cataliotti, L. Fallani, F. Ferlaino, P. Maddaloni, and M. Inguscio, Phys. Rev. Lett. **90**, 140405 (2003).
[21] In addition, the chemical potential must be smaller than the energy splitting $\hbar\omega_L$. With typical parameters this condition is always met as long as the chemical potential is much smaller than the lattice depth.
[22] D. van Oosten, P. van der Straten, and H.T.C. Stoof, Phys. Rev. A **67**, 033606 (2003).
[23] Y. Kagan, E.L. Surkov, and G.V. Shlyapnikov, Phys. Rev. A **55**, R18 (1997).
[24] D.S. Jin, J.R. Ensher, M.R. Matthews, C.E. Wieman, and E. Cornell, Phys. Rev. Lett. **77**, 420 (1996).
[25] M. Edwards, P.A. Ruprecht, K. Burnett, R.J. Dodd, and C.W. Clark, Phys. Rev. Lett. **77**, 1671 (1996).
[26] U.A. Khawaja and H. Stoof, Phys. Rev. A **65**, 013605 (2001).
[27] K.W. Madison, F. Chevy, W. Wohlleben, and J. Dalibard, Phys. Rev. Lett. **86**, 4443 (2001).
[28] E. Hodby, G. Hechenblaikner, S.A. Hopkins, O.M. Maragó, and C.J. Foot, Phys. Rev. Lett. **88**, 010405 (2002).
[29] D.L. Feder, C.W. Clark, and B.I. Schneider, Phys. Rev. Lett. **82**, 4956 (1999).
[30] A. Recati, F. Zambelli, and S. Stringari, Phys. Rev. Lett. **86**, 377 (2001).
[31] S. Sinha and Y. Castin, Phys. Rev. Lett. **87**, 190402 (2001).
[32] R.J. Dodd, K. Burnett, M. Edwards, and C.W. Clark, Phys. Rev. A **56**, 587 (1997).
[33] F. Zambelli and S. Stringari, Phys. Rev. Lett. **81**, 1754 (1998).
[34] A MATHEMATICA file containing the relevant Lagrangian and the solution for the quadrupole mode frequencies can be downloaded from URL http://www.phys.uu.nl/~martiknn/BEC_In_1DLattice.html
[35] J.O. Andersen, U.A. Khawaja, and H.T.C. Stoof, Phys. Rev. Lett. **88**, 070407 (2002).
[36] U.A. Khawaja, J.O. Andersen, N.P. Proukakis, and H.T.C. Stoof, Phys. Rev. A **66**, 013615 (2002).
[37] U.A. Khawaja, N.P. Proukakis, J.O. Andersen, M.W.J. Romans, and H.T.C. Stoof, e-print cond-mat/0303485.
[38] J. Javanainen, Phys. Rev. A **60**, 4902 (1999).